1. Materials

All chemicals and solvents were purchased from Sigma Aldrich, SAMCHUN or Alfa Aesar and used without further purification.

2. Experimental procedures

Cycloocta[1,2-c3,4-c'5,6-c''7,8-c''']tetrafuran, 1: The synthesis was performed using a previously reported literature report.[1] ^{1}H NMR (300 MHz, $CDCl_3$, 298 K): δ 7.20 (s, 8H, Ar-H).

(1R,4S,5S,8R)-1,4,5,8-Tetrahydro-1,4:5,8-diepoxyanthracene, 2: The synthesis was performed using a previously reported literature report.[2] ^{1}H NMR (300 MHz, $CDCl_3$, 298 K): δ 5.63 (d, 4H, OCH), 7.03 (dd, 4H, C=CH), 7.20 (s, 2H, Ar-H).

3D ep-POP: The synthesis was performed using previously reported literature procedure.[3] FT-IR (powder): 2970, 2926, 2855, 1444, 1382, 1336, 1111, 1003, 929, 852, 697, 604 cm^{-1}. Anal. calcd. for $C_{44}H_{28}O_8$: C, 77.18; H, 4.12; O, 18.69. Found: C, 77.13; H, 4.19; O, 18.68.

3D p-POP: 3D ep-POP (50 mg) was added into a flame-dried 10-ml round-bottomed flask in Ar atmosphere. A mixture of methanesulfonic acid (0.08 ml, 1.23 mmol) and acetic anhydride (0.1 ml, 1.06 mmol) in dry dioxane (5 mL) was added to the flask. After stirring for 3 hours, the reaction was heated up to 90°C overnight. The product was filtered and washed with H_2O (2 x 100 mL), methanol (2 x 100 mL), chloroform (2 x 100 mL), and acetone (2 x 100 mL) and soxhleted in THF for 5 days. The **3D p-POP** powder was obtained after drying under vacuum at 120°C for 6 h. FT-IR (powder): 2126, 1661, 1603, 1456, 1225, 1163, 1048, 1002, 907, 878, 762, 731cm^{-1}. Anal. calcd. for $C_{44}H_{20}$: C, 96.33; H, 3.67. Found: C, 96.29; H, 3.71.

I_2@3D p-POP: 3D p-POP (10 mg) was added to a 20 mL open scintillation vial, which was placed in a capped 50 mL jar containing 120 mg of I_2 at 296 K for 16 hours. For VT conductivity and XPS measurements, the powder was evacuated under dynamic vacuum for 8 hours to remove residual unreacted I_2.

3. Characterization methods

Characterization. Solid-state CP/MAS **^{13}C NMR** spectra was analyzed using Bruker Avance 400 MHz NMR instrument. X-ray photoelectron spectroscopy (**XPS**) analysis was obtained from a multi-purpose XPS (Sigma Probe or K-Alpha+, Thermo VG Scientific, X-ray Source:

monochromatic Al K-alpha). **FT-IR** spectra was performed on Shimatzu IRTracer-100. **Raman** spectroscopy was obtained using 235 nm laser excitation source with a Horiba Jobin-Yvon LabRAM HR confocal Raman microscope. Ar adsorption and desorption isotherms were obtained at 87 K on a **Micromeritics** 3Flex Surface Characterization Analyzer. All samples were outgassed at 100°C for 6 h prior to the analysis. Powder X-ray diffraction (**PXRD**) patterns of the polymers with 2θ ranging from 5 to 80° were performed using a Rigaku D/MAX-2500 Multi-purpose High Power X-ray diffractometer. The morphology of 3D ep-POP and p-POP was investigated using a field emission scanning electron microscope (**FE-SEM**, Sirion). Elemental compositions of the polymers were analyzed using FlashEA 2000 Series [C, H, N] Elemental Analyzer. Thermogravimetric analysis (**TGA**) was obtained with a Netzsch-TG 209 F3 or TA Instruments Q500 Thermogravimetric Analyzer at a heating rate of 2°C min^{-1} up to 800°C under air. **Room temperature conductivity** measurements were carried out at 296 K in ambient atmosphere on three pressed pellets each of 3D ep-POP and p-POP using a home-built two-probe in situ press set-up described previously[4]. Linear *I–V* curves were obtained by sweeping the voltage between –0.5 and +0.5 V and measuring the current using a sourcemeter (Keithley 2450) connected to the press via test leads. Pellet thicknesses were measured after the measurement using a micrometer (Mitutoyo). **Variable temperature conductivity** measurements were carried out in a home-built two-probe in situ screw press set-up described previously[5]. Electrical contacts were made by touching the short screw or the inner plate of the sample mounting chuck by gold-coated tungsten probes. Probes were connected to a sourcemeter (Keithley model 2450) through triax cables. Temperature was balanced by the heater of the probe station chuck and liquid nitrogen and was regulated by a temperature controller (Scientific Instruments 9700). All measurements were performed under dynamic vacuum (~1×10^{-5} Torr). *I–V* curves were collected by sweeping voltage while scanning temperatures with a step size of 10 K and 30 minutes per step. The final measurement at each temperature was used as the conductance of the device. **Diffuse reflectance UV-Vis-NIR** spectra were collected between 400 and 2500 nm at a scan rate of 400 nm/min using a PIKE Technologies DiffusIR accessory in a Cary 5000i spectrophotometer. 3D p-POP and I_2@3D p-POP were ground with KBr in a mortar and pestle to a 1 wt% dilution. Spectra were normalized to a 100% KBr baseline, and the Kubelka–Munk equation was applied ($F(R) = \frac{(1-R)^2}{2R}$). The Kubelka–Munk function-transformed spectra were then normalized with respect to $F(R)$ at 475 nm (21,000 cm^{-1}). **Diffuse reflectance infrared Fourier transform spectroscopy (DRIFTS)**

measurements were collected on a Bruker Tensor 37 using a PIKE Technologies DiffusIR accessory. 3D p-POP and I_2@3D p-POP were ground with KBr in a mortar and pestle to a 2.5 wt% dilution. Data were averaged over 16 scans between 4000 and 600 cm^{-1}. Each of the Kubelka-Munk function-transformed DRIFTS spectra were normalized with respect to the DRUV–vis–NIR data by matching the DRIFTS value of $F(R)$ at 4000 cm^{-1} with the DRUV–vis–NIR value of $F(R)$ of the same sample at 4000 cm^{-1}.

4. Characterization of 3D ep-POP and 3D p-POP

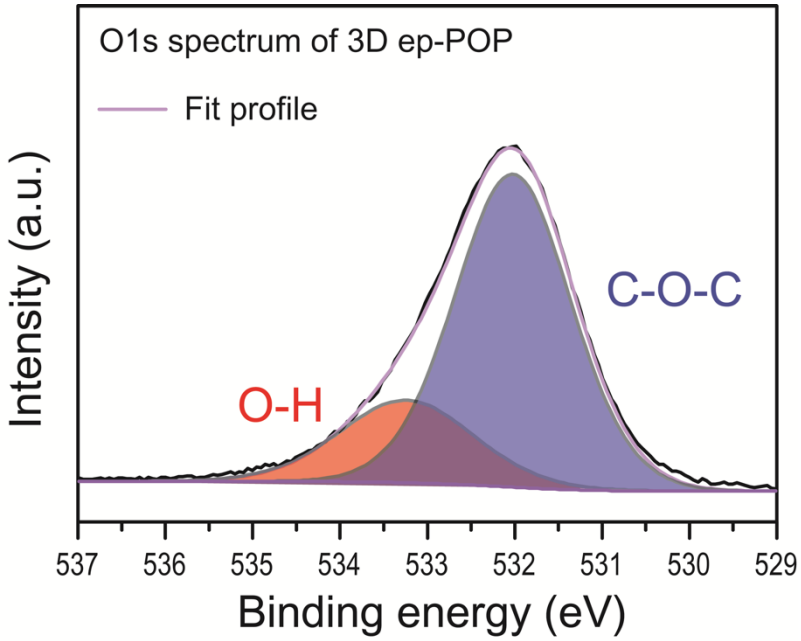

Figure S1. O1s XPS analysis of 3D ep-POP.

Table S1. C 1s binding energy and surface concentration from the XPS spectra of 3D ep-POP and 3D p-POP.

Binding Energy (eV)	Chemical Bonds	Concentration %	
		3D ep-POP	3D p-POP
284.5	C=C	59.9	68.32
285.6	C-C	16.8	-
286.4	C-O-C / C-O-H	19.2	20.09
288.6	C-O	4.1	11.58

Table S2. O 1s binding energy and surface concentration from the XPS spectra of 3D ep-POP.

Binding Energy (eV)	Chemical Bonds	Concentration %
532.0	C-O-C	76.3
533.5	O-H	23.7

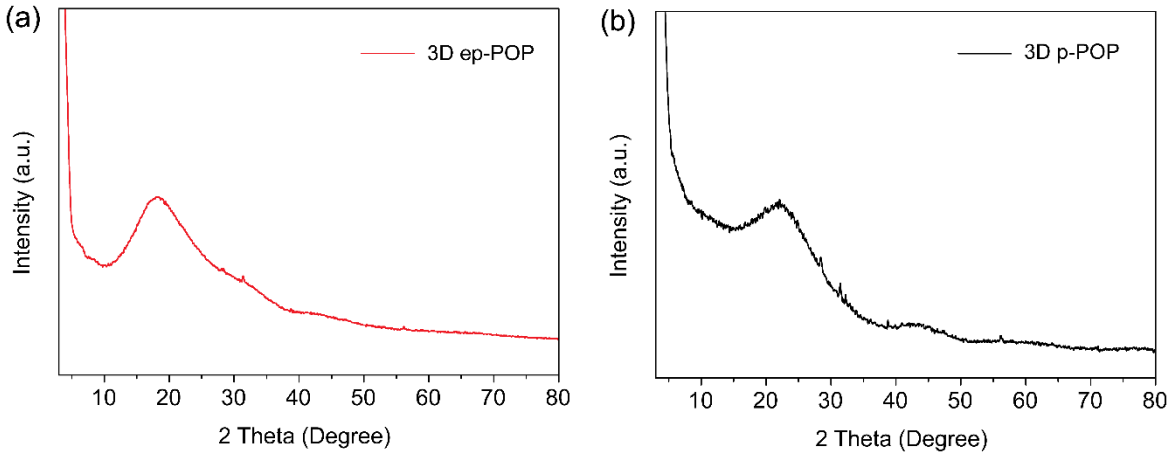

Figure S2. Powder X-ray diffraction (PXRD) patterns of 3D ep-POP and 3D p-POP in the 2θ range of 3 to 80°.

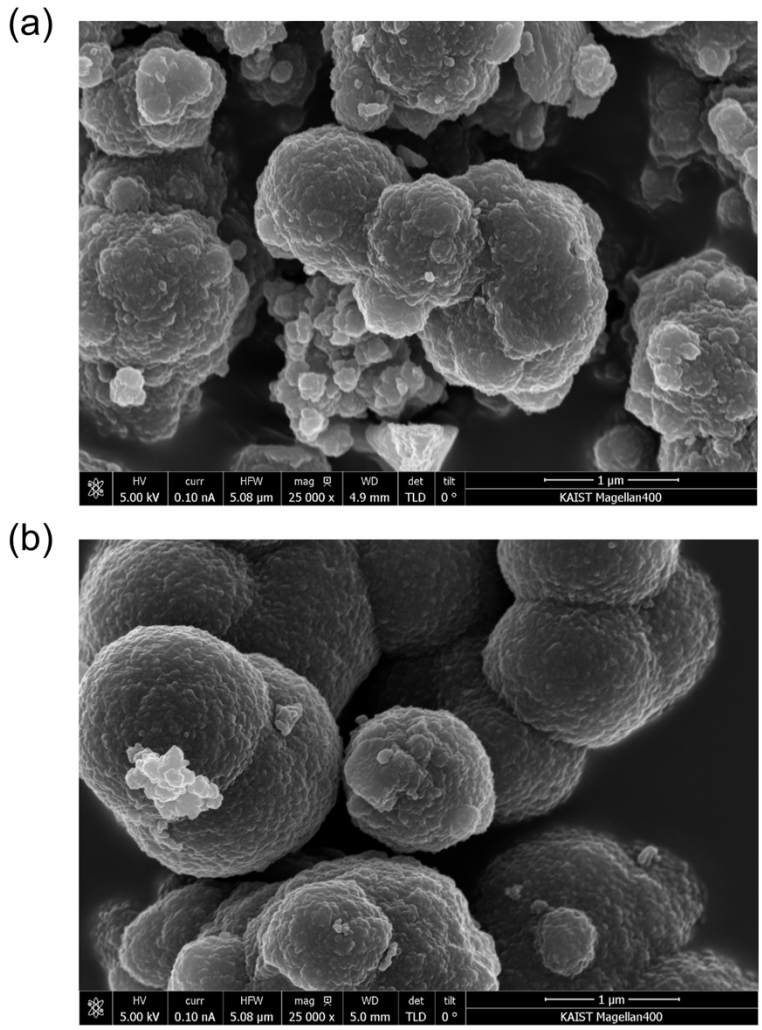

Figure S3. FE-SEM images of (a) 3D ep-POP and (b) 3D p-POP.

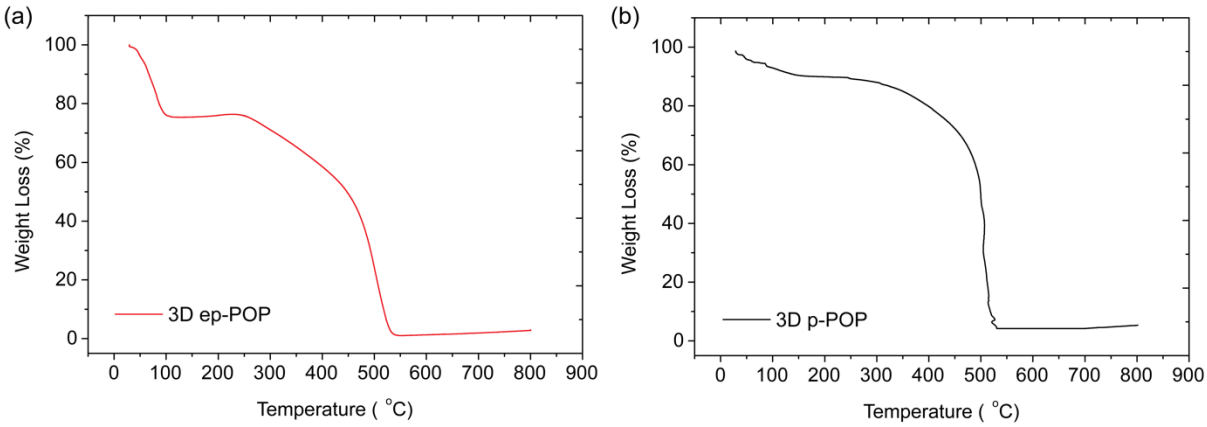

Figure S4. Thermogravimetric analyses of (a) 3D ep-POP and (b) 3D p-POP under air atmosphere.

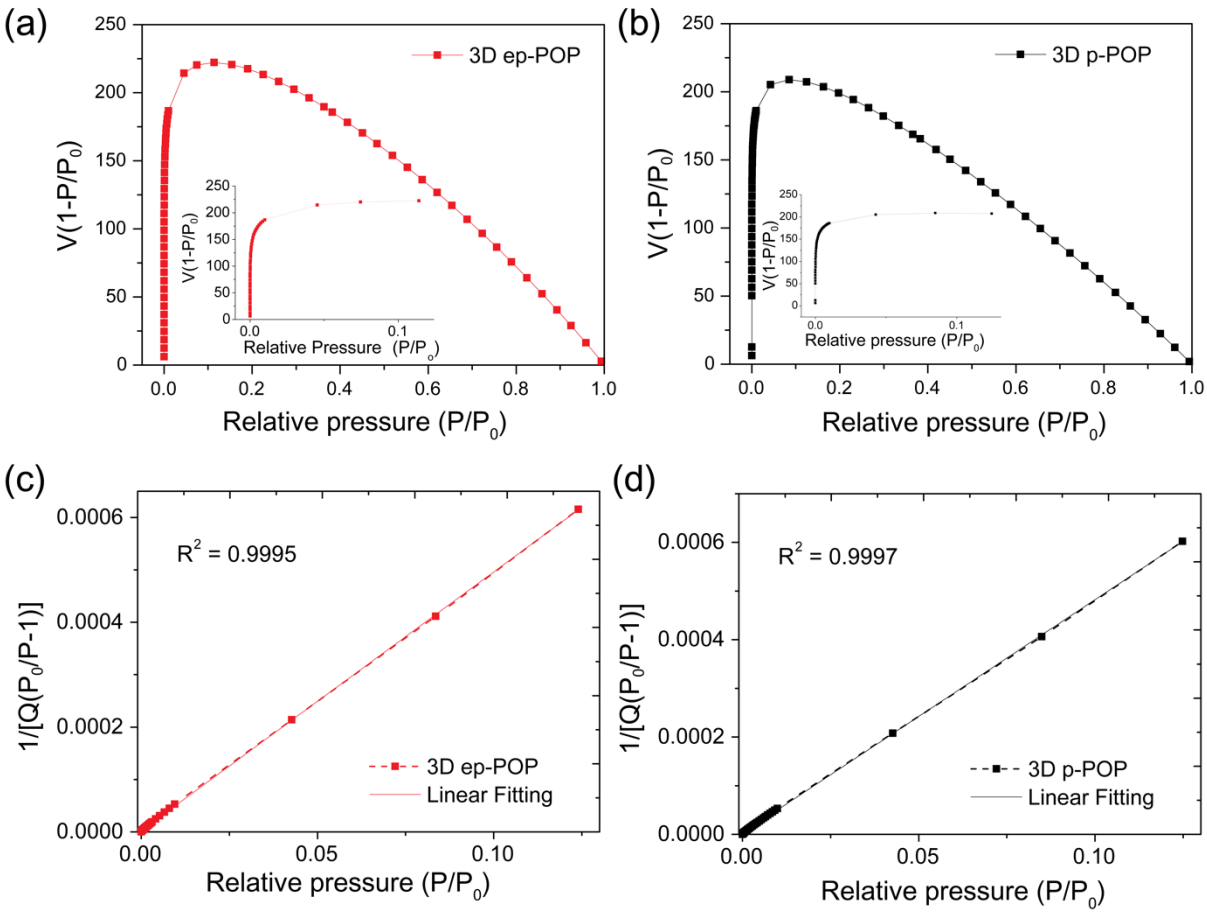

Figure S5. Calculated Rouquerol plots of (a) 3D ep-POP and (b) 3D p-POP (Inset: Expanded P/P_0 region used for the BET surface area calculations). For surface area calculations, we selected the pressure range up to $P/P_0 = 0.1$ where the term $V(1-P/P_0)$ continuously increases with P/P_0. BET linear plots of (c) 3D ep-POP and (b) 3D p-POP obtained from Ar isotherms at 87 K.

Table S3. BET surface areas and conductivities of 3D ep-POP and 3D p-POP.

Polymer	S_{BET} (m^2 g^{-1})	S_{micro} (m^2 g^{-1})	Langmuir (m^2 g^{-1})	V_{micro} (cm^3 g^{-1})	d_{micro} (nm)	Conductivity at 296 K (S cm^{-1})
3D ep-POP	779	462	936	0.17	0.40	$8(1) \times 10^{-10}$
3D p-POP	801	501	965	0.19	0.41	$5(3) \times 10^{-8}$

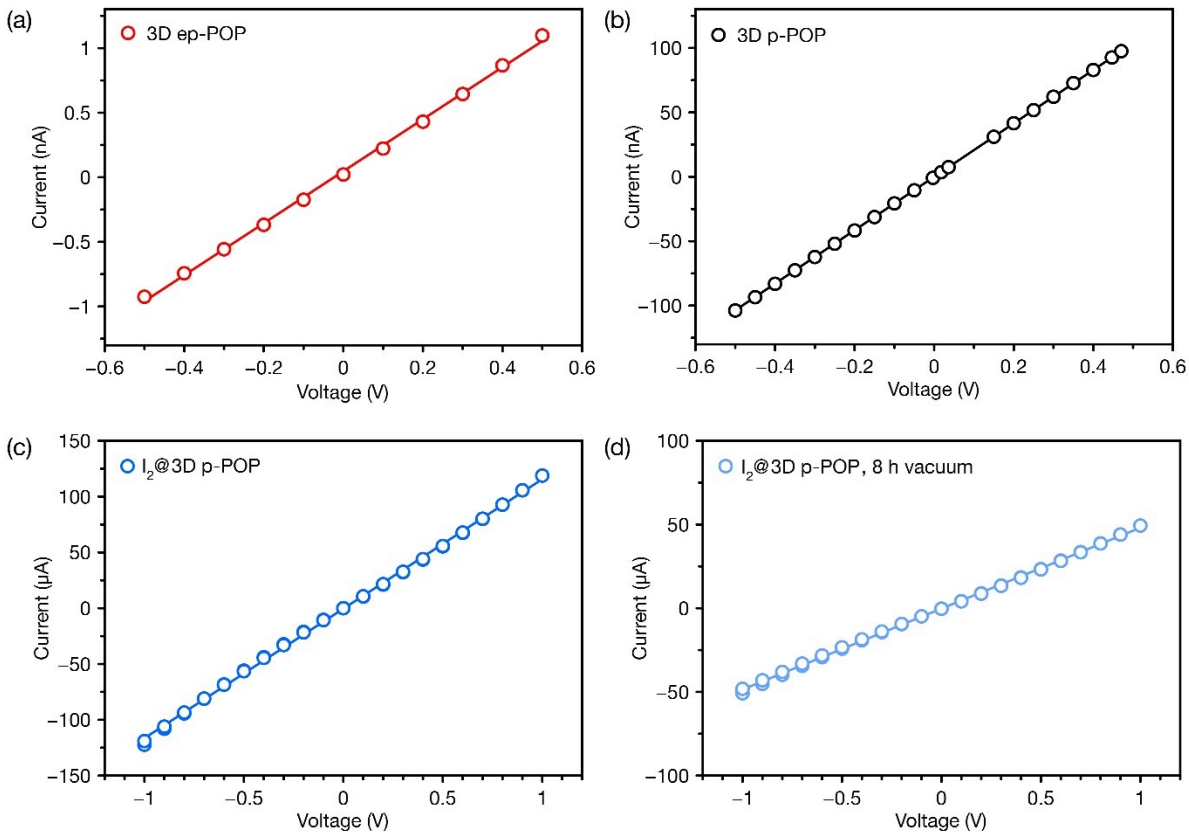

Figure S6. Representative *I–V* curves for two-probe pressed pellets of (a) 3D ep-POP, (b) 3D p-POP, (c) I_2@3D p-POP, and (d) I_2@3D p-POP after 8 h exposure to vacuum, taken at room temperature (296 K). The solid lines correspond to linear fits to the data.

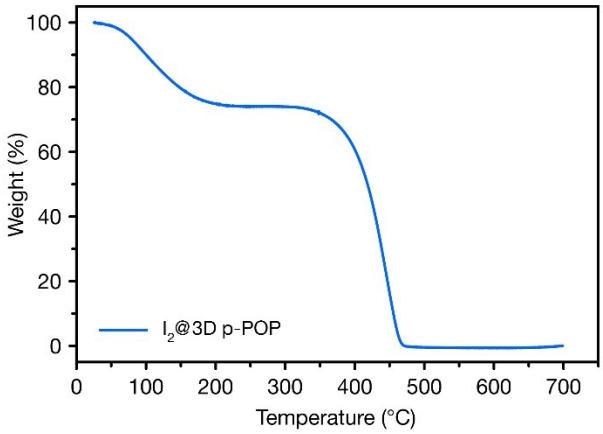

Figure S7. Thermogravimetric analysis of I_2@3D p-POP under air atmosphere.

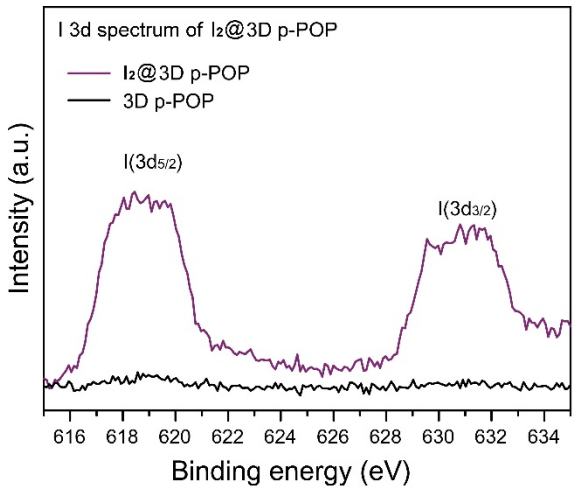

Figure S8. I 3d XPS analysis of 3D p-POP and I_2@3D p-POP.

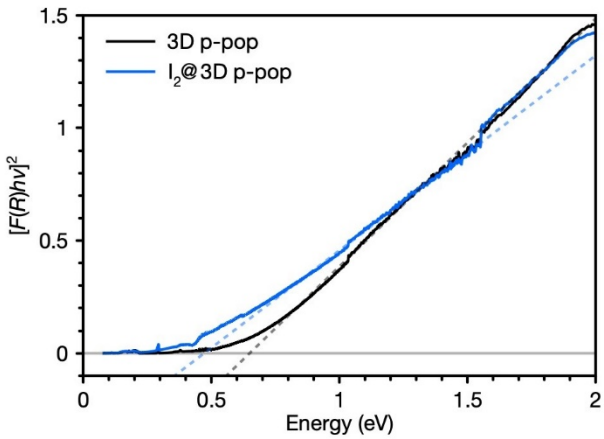

Figure S9. Tauc plot of DRIFTS and UV-vis-NIR data for 3D p-POP and I_2@3D p-POP.

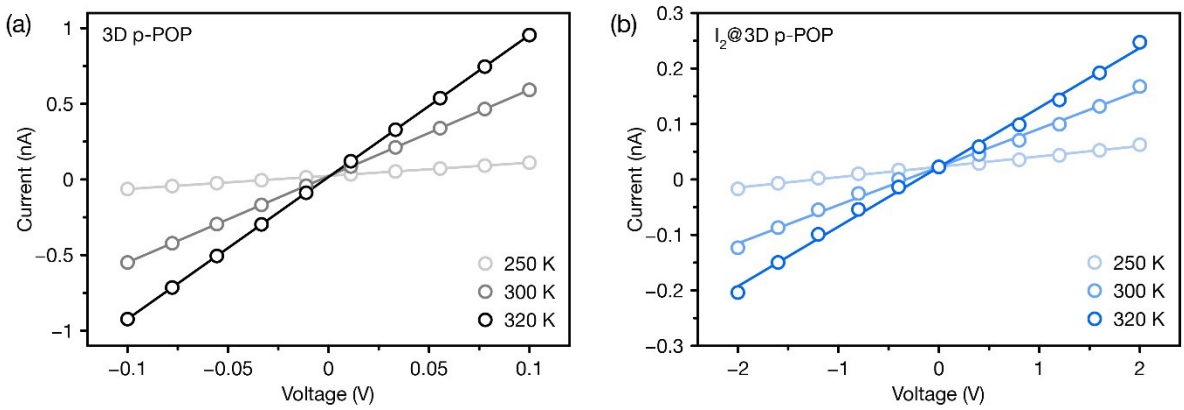

Figure S10. *I–V* curves for a two-probe pressed pellet of (a) 3D p-POP and (b) I_2@3D p-POP taken at different temperatures. The solid lines correspond to linear fits to the data.

Table S4. Comparison of conductivities and surface areas of selected porous organic polymers and framework materials.

Polymer	Conductivity (S cm^{-1})	BET surface area (m^2 g^{-1})	Reference
3D ep-POP	$8(1) \times 10^{-10}$	779	This work
3D p-POP	$5(3) \times 10^{-8}$	801	This work
I_2@3D p-POP	$6(2) \times 10^{-4}$	–	This work
JUC-Z2*	$\sim 3 \times 10^{-7}$	2081	[6]
I_2@JUC-Z2*	$\sim 1 \times 10^{-1}$	–	[6]
POP-1	2.1×10^{-3}	260	[7]
POP-2	6.7×10^{-3}	342	[7]
sp^{2}c-COF	6.1×10^{-16}	692	[8]
I_2@sp^{2}c-COF	7.1×10^{-4}	–	[8]
TTF-Ph-COF	10^{-5}	1014	[9]
TTF-Py-COF	10^{-6}	817	[9]

5. References

[1] T. Fallon, A. C. Willis, A. D. Rae, M. N. Paddon-Row, M. S. Sherburn, *Chem. Sci.* **2012**, *3*, 2133-2137.

[2] P. R. Ashton, G. R. Brown, N. S. Isaacs, D. Giuffrida, F. H. Kohnke, J. P. Mathias, A. M. Z. Slawin, D. R. Smith, J. F. Stoddart, D. J. Williams, *J. Am. Chem. Soc.* **1992**, *114*, 6330-6353.

[3] Y. Byun, A. Coskun, *Angew. Chem. Int. Ed.* **2018**, *57*, 3173-3177.

[4] L. Sun, S. S. Park, D. Sheberla, M. Dincă, *J. Am. Chem. Soc.* **2016**, *138*, 14772-14782.

[5] L. Sun, C. H. Hendon, S. S. Park, Y. Tulchinsky, R. Wan, F. Wang, A. Walsh, M. Dinca, *Chem. Sci.* **2017**, *8*, 4450-4457.

[6] T. Ben, K. Shi, Y. Cui, C. Pei, Y. Zuo, H. Guo, D. Zhang, J. Xu, F. Deng, Z. Tian, S. Qiu, *J. Mater. Chem.* **2011**, *21*, 18208-18214.

[7] T. Li, W. Zhu, R. Shen, H.-Y. Wang, W. Chen, S.-J. Hao, Y. Li, Z.-G. Gu, Z. Li, *New J. Chem.* **2018**, *42*, 6247-6255.

[8] E. Jin, M. Asada, Q. Xu, S. Dalapati, M. A. Addicoat, M. A. Brady, H. Xu, T. Nakamura, T. Heine, Q. Chen, D. Jiang, *Science* **2017**, *357*, 673-676.
[9] S. Jin, T. Sakurai, T. Kowalczyk, S. Dalapati, F. Xu, H. Wei, X. Chen, J. Gao, S. Seki, S. Irle, D. Jiang, *Chem. Eur. J.* **2014**, *20*, 14608-14613.